polymer papers

Morphology predictions for ternary polymer blends undergoing spinodal decomposition

E. Bruce Nauman* and David Qiwei He
The Isermann Department of Chemical Engineering, Rensselaer Polytechnic Institute, Troy, NY 12180-3590, USA
(Received 23 July 1993)

Spinodal decomposition has been simulated in two spatial dimensions for ternary polymer mixtures over a wide range of volume fractions and Flory–Huggins interaction parameters. A great wealth of morphologies was observed: some closely approximate morphologies seen in cast film experiments, while others invite experimental confirmation. A taxonomy of phase structures is proposed.

(Keywords: morphology; ternary polymer blends; spinodal decomposition)

INTRODUCTION

Multiphase blends consisting of two or more incompatible polymers have achieved major economic importance in the plastics industry. The most widespread examples are impact modified thermoplastics where a rubber is microdispersed in a glassy polymer matrix. Some materials are reported to have co-continuous phases of different thermoplastics[1]. Most commercial materials have two phases and are formed from two main polymers with minor amounts of a third, compatibilizing polymer, typically a graft or block copolymer. These materials can be made by a variety of methods including chemical routes such as precipitation polymerization. However, much interest has focused on strictly physical routes such as extruder compounding or compositional quenching[2]. The resulting structures are not in thermodynamic equilibrium but may be sufficiently stable for practical use.

The present paper explores the morphologies possible with three mutually incompatible polymers. The results apply when a single-phase mixture is rapidly quenched into an unstable region so that phase separation occurs by spinodal decomposition. Typically, there will be three separate phases corresponding to the three component polymers.

Thermal quenching is rarely possible in polymer systems because the upper solubility temperature exceeds the thermal stability limits of the components. Bulk samples can be prepared by compositional quenching where a compatibilizing solvent is rapidly removed by flash devolatilization or by antisolvent coagulation where the solvent removal rate is appreciably slower. Thin films can be made by solvent casting, and the structures observed in such films motivated the present study. *Figure 1* shows a two-dimensional structure obtained when 55 wt% polystyrene and 45 wt% poly(methyl methacrylate) was cast from a tetrahydrofuran solution. The semicontinuous phase would presumably be co-continuous in three dimensions. (In fact, hydrodynamic instabilities tend to give particulate structures in three dimensions[3–5]. Hydrodynamics are negligible in thin films). *Figure 2* shows a similarly cast film containing 50% polystyrene, 40% poly(methyl methacrylate) and 10% polybutadiene. The semicontinuous nature of the two major phases is maintained but a third, polybutadiene phase appears as particulates within the polystyrene phase. *Figure 3* shows the cast film that resulted when poly(methyl methacrylate) constituted 50 wt%, polystyrene 40 wt% and polybutadiene 10 wt%. Although somewhat ambiguous, this structure appears to have a continuous poly(methyl methacrylate) phase and a dispersed phase consisting of polystyrene and polybutadiene in a core–shell structure. In the following, we shall attempt to explain such morphologies and to illustrate other morphologies possible in ternary polymer blends.

THEORY

The approach generally follows that of Nauman and Balsara[6]. The free energy of mixing depends on component concentrations and also on gradients in concentration. The total free energy of the system is given by:

$$G_{\text{total}} = \int_v G(a, b, c, \nabla a, \nabla b, \nabla c)\, dv \qquad (1)$$

where a, b, c are mole, weight or volume fractions depending on the specific application and v is the system volume. They are subject to the constraint that

$$a + b + c = 1 \qquad (2)$$

but we do not yet use this relationship to eliminate one of a, b or c. Instead, all three are retained as quasi-independent variables.

* To whom correspondence should be addressed

0032-3861/94/11/2243-13

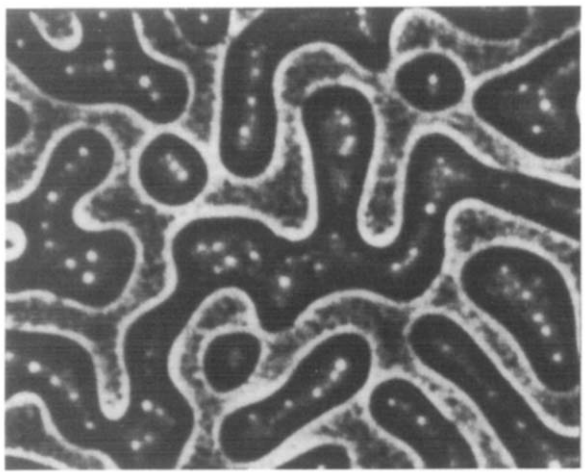

Figure 1 Cast film containing 55% polystyrene, 45% poly(methyl methacrylate)

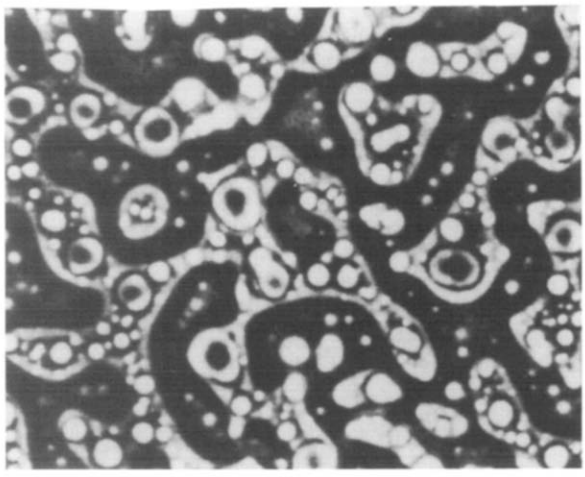

Figure 2 Cast film containing 50% polystyrene, 40% poly(methyl methacrylate), 10% polybutadiene

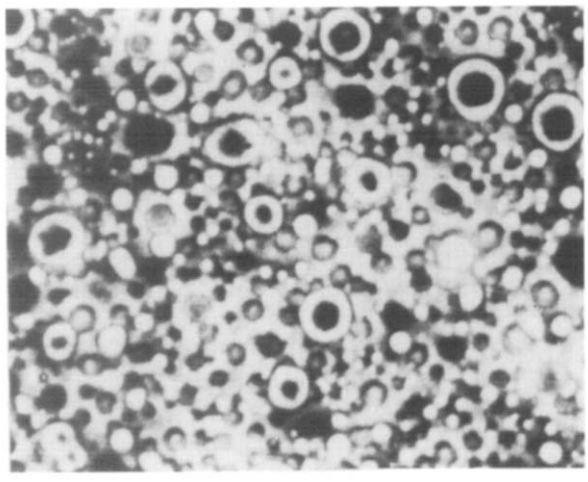

Figure 3 Cast film containing 40% polystyrene, 50% poly(methyl methacrylate), 10% polybutadiene

Nauman and Balsara[6] used equation (1) to define a variational free energy, Ψ, by:

$$\left(\frac{\partial\Psi}{\partial a}\right)_{b,c}=\left(\frac{\delta G_{\text{total}}}{\delta a}\right)_{b,c}=\left(\frac{\partial G}{\partial a}\right)_{b,c,\nabla a,\nabla b,\nabla c}-\nabla\cdot\left(\frac{\partial G}{\partial\nabla a}\right)_{a,b,c,\nabla b,\nabla c} \tag{3}$$

with similar equations for $\partial\Psi/\partial b$ and $\partial\Psi/\partial c$. The generalized chemical potential is defined as:

$$\mu_A=\Psi+(b+c)\left(\frac{\partial\Psi}{\partial a}\right)_{b,c}-b\left(\frac{\partial\Psi}{\partial b}\right)_{a,c}-c\left(\frac{\partial\Psi}{\partial c}\right)_{a,b} \tag{4}$$

with similar equations for μ_B and μ_C. The variational free energy and the generalized chemical potentials are functions of state at equilibrium[7]. In a non-equilibrium situation, gradients of the generalized chemical potential provide the driving force for diffusion. Following Cussler[8] and others, we write

$$-j_A=Da\nabla\mu_A \tag{5}$$

where j_A is the flux of component A. Similar equations hold for components B and C. It is assumed here that D is a constant, independent of concentration and identical for all species. Cross diffusion — where a flux of component A is induced by gradients in μ_B or μ_C — is ignored.

It is then true that:

$$-j_A=abD\nabla(\mu_A-\mu_B)+acD\nabla(\mu_A-\mu_C) \tag{6a}$$

$$-j_B=abD\nabla(\mu_B-\mu_A)+bcD\nabla(\mu_B-\mu_C) \tag{6b}$$

$$-j_C=acD\nabla(\mu_C-\mu_A)+bcD\nabla(\mu_C-\mu_B) \tag{6c}$$

where $j_A+j_B+j_C=0$. The chemical potential differences are evaluated using equation (4):

$$\mu_A-\mu_B=\frac{\partial\Psi}{\partial a}-\frac{\partial\Psi}{\partial b} \tag{7a}$$

$$\mu_A-\mu_C=\frac{\partial\Psi}{\partial a}-\frac{\partial\Psi}{\partial c} \tag{7b}$$

$$\mu_B-\mu_C=\frac{\partial\Psi}{\partial b}-\frac{\partial\Psi}{\partial c} \tag{7c}$$

It will be seen that these differences are defined under non-equilibrium conditions. Thus the formal difficulty of basing a (necessarily non-equilibrium) diffusive flux on a quantity defined only at equilibrium is avoided.

A general form for the function G in equation (1) is:

$$G=g(a,b,c)+\tfrac{1}{2}\kappa_{AA}(\nabla a)^2+\tfrac{1}{2}\kappa_{BB}(\nabla b)^2+\tfrac{1}{2}\kappa_{CC}(\nabla c)^2+\kappa_{AB}\nabla a\nabla b+\kappa_{AC}\nabla a\nabla c+\kappa_{BC}\nabla b\nabla c \tag{8}$$

where $g(a,b,c)$ is the (ordinary) free energy of mixing and the κ are gradient energy parameters according to the formulation of Cahn and Hilliard[9]. Substituting $c=1-a-b$ into the gradient terms gives:

$$G=g(a,b,c)+\frac{\kappa_1}{2}(\nabla a)^2+\kappa_{12}\nabla a\nabla b+\frac{\kappa_2}{2}(\nabla b)^2 \tag{9}$$

where $\kappa_1=\kappa_{AA}+\kappa_{CC}-2\kappa_{AC}$, $\kappa_2=\kappa_{BB}+\kappa_{CC}-2\kappa_{BC}$ and $\kappa_{12}=\kappa_{CC}+\kappa_{AB}-\kappa_{AC}-\kappa_{BC}$. Equation (9) is the form encountered in the literature for which estimates of the κ have been made[10]. We use it here and thus depart from complete symmetry with respect to the three species.

A regular solution of Flory–Huggins form is used for the ordinary free energy:

$$g=\frac{a\ln a}{n_A}+\frac{b\ln b}{n_B}+\frac{c\ln c}{n_C}+\chi_{AB}ab+\chi_{AC}ac+\chi_{BC}bc \tag{10}$$

where χ_{AB}, χ_{AC} and χ_{BC} are binary interaction coefficients and the n are chain lengths for the polymers.

Established theory suggests that the χ are functions of temperature and that the κ are functions of temperature and composition[10,11]. For spinodal decomposition under isothermal conditions, equation (7) becomes:

$$\mu_A-\mu_B=\frac{\partial g}{\partial a}-\frac{\partial g}{\partial b}-\nabla(\kappa_1-\kappa_{12})\nabla a+\nabla(\kappa_2-\kappa_{12})\nabla b+\left(\frac{\partial\kappa_1}{\partial a}-\frac{\partial\kappa_1}{\partial b}\right)\frac{(\nabla a)^2}{2}+\left(\frac{\partial\kappa_{12}}{\partial a}-\frac{\partial\kappa_{12}}{\partial b}\right)\nabla a\nabla b+\left(\frac{\partial\kappa_2}{\partial a}-\frac{\partial\kappa_2}{\partial b}\right)\frac{(\nabla b)^2}{2} \tag{11}$$

$$\mu_A-\mu_C=\frac{\partial g}{\partial a}-\frac{\partial g}{\partial c}-\nabla\kappa_1\nabla a-\nabla\kappa_{12}\nabla b+\frac{\partial\kappa_1}{\partial a}\frac{(\nabla a)^2}{2}+\frac{\partial\kappa_{12}}{\partial a}\nabla a\nabla b+\frac{\partial\kappa_2}{\partial a}(\nabla b)^2 \tag{12}$$

$$\mu_B-\mu_C=\frac{\partial g}{\partial b}-\frac{\partial g}{\partial c}-\nabla\kappa_2\nabla b-\nabla\kappa_{12}\nabla a+\frac{\partial\kappa_1}{\partial a}\frac{(\nabla a)^2}{2}+\frac{\partial\kappa_{12}}{\partial b}+\nabla a\nabla b+\frac{\partial\kappa_2}{\partial b}(\nabla b)^2 \tag{13}$$

In this formulation, we have supposed the κ to be functions of a and b only.

Computations become much simpler when the compositional dependence of the κ is ignored. The component continuity equations then become:

$$\frac{\partial a}{\partial t}=\nabla abD\nabla(\mu_A-\mu_B)+\nabla acD\nabla(\mu_A-\mu_C)$$

$$=D\nabla\left\{ab\nabla\left[\frac{\partial g}{\partial a}-\frac{\partial g}{\partial b}-(\kappa_1-\kappa_{12})\nabla^2a+(\kappa_2-\kappa_{12})\nabla^2b\right]+ac\nabla\left(\frac{\partial g}{\partial a}-\frac{\partial g}{\partial c}-\kappa_1\nabla^2a-\kappa_{12}\nabla^2b\right)\right\} \tag{14}$$

$$\frac{\partial b}{\partial t}=\nabla abD\nabla(\mu_B-\mu_A)+\nabla bcD\nabla(\mu_B-\mu_C)$$

$$=D\nabla\left\{ab\nabla\left[-\frac{\partial g}{\partial a}+\frac{\partial g}{\partial b}+(\kappa_1-\kappa_{12})\nabla^2a-(\kappa_2-\kappa_{12})\nabla^2b\right]+bc\nabla\left(\frac{\partial g}{\partial b}-\frac{\partial g}{\partial c}-\kappa_2\nabla^2b-\kappa_{12}\nabla^2a\right)\right\} \tag{15}$$

Ignoring the compositional dependence of κ is equivalent to ignoring its entropic component and is justified in the limit of high molecular weight. We suppose that the three polymers have similar and large radii of gyration. Then, with the length coordinate scaled using the common radius of gyration, R_g, the enthalpic components of the κ are given by:

$$\kappa_1=\frac{2\chi_{AC}}{3} \tag{16}$$

$$\kappa_2=\frac{2\chi_{BC}}{3} \tag{17}$$

$$\kappa_{12}=\frac{\chi_{AC}+\chi_{BC}-\chi_{AB}}{3} \tag{18}$$

Thus, in the limit of high molecular weight, the κ depends only on the χ, and equations (14) and (15) contain only the χ and the diffusivity, D, as physical parameters. A scaled time coordinate

$$\tau=\frac{Dt}{R_g^2} \tag{19}$$

eliminates D as a simulation parameter.

The spinodal region of the ternary system can be determined from:

$$S=\frac{1}{\bar a\bar c n_A n_B}+\frac{1}{\bar a\bar c n_A n_C}+\frac{1}{\bar b\bar c n_B n_C}-2\left(\frac{\chi_{AB}}{\bar c n_C}+\frac{\chi_{AC}}{\bar b n_B}+\frac{\chi_{BC}}{\bar a n_A}\right)-\chi_{AB}^2-\chi_{BC}^2-\chi_{AC}^2+2\chi_{AB}\chi_{BC}+2\chi_{AB}\chi_{AC}+2\chi_{AC}\chi_{BC} \tag{20}$$

where $\bar a$, $\bar b$ and $\bar c=1-\bar a-\bar b$ are the system average concentrations.

This result is consistent with those of Scott[12] and Tompa[13] but has been derived for a free energy function expressed in volume (or mole) fractions rather than absolute numbers of moles. Also, as written above, it explicitly shows the stability criterion to be invariant with respect to the choice of dependent concentration variable. When $S<0$, an initially mixed system is within the spinodal region and will spontaneously separate into two or three phases. When $S>0$, the system is usually stable or metastable so that spinodal decomposition will not occur. However, equation (20) can give false positives with $S>0$ for systems that are in fact unstable. The ancillary condition

$$S_A=\frac{1}{\bar a n_A}+\frac{1}{\bar c n_C}-2\chi_{AC}\geqslant 0 \tag{21}$$

removes these false positives. The system is within the spinodal if either $S<0$ or $S_A<0$.

The number of phases, the phase morphology and the average phase compositions have limiting values at equilibrium. However, the microseparated systems considered in this paper have not achieved equilibrium, and the determination of the equilibrium concentrations will not be explicitly treated here. As a practical matter, the phase morphologies that result from spinodal decomposition are dramatically different from the two or three fully separated layers that correspond to global equilibrium. The concentrations within the microseparated domains approach the equilibrium (binodal) concentrations, but a measurable fraction of the system is interfacial material having intermediate concentrations. A phase exists when the volume fraction of a component exceeds 0.5. Following this definition, a ternary system may possess regions that belong to no phase.

A substantial simplification of the governing equations results from assuming $n_A=n_B=n_C=n$ and by multiplying equations (14) and (15) by n. In effect, this drops the reciprocal n terms from equations (10) and (16) and replaces each of the χ terms by $n\chi$. The dimensionless time becomes:

$$\tau=\frac{Dt}{nR_g^2} \tag{22}$$

In what follows, the term $n\chi$ will be replaced by χ.

Numerical studies

Equations (14) and (15) were solved using a fully explicit, finite difference approach. The initial conditions corresponded to a nearly homogeneous mixture of

profiles, the morphology is invariant (self-similar) with time, and the domain sizes grow as the cube root of time. For a polymer with $n=1000$, $R_g=200$ Å and $D=10^{-11}$ m^2 s^{-1}, $\tau=400$ corresponds to 16 s.

More than 200 simulation runs were made to systematically explore the effects of phase volume and interaction parameters. The interaction parameters were chosen from the set $\chi=3, 4.5, 6, 9$.

The numerical results of the simulations were graphically displayed using several visualization techniques. The most generally useful method assigned a primary colour (blue, green or red) to each pure component. A single graph was produced with the colour assigned to each pixel being a sum — weighted according to the component concentrations — of the primary colours. *Plates 1–21* utilize this technique.

Another visualization method was particularly useful for distinguishing whether a minor component was locally enriched in concentration or had developed as a separate phase. This method used separate plots for each component and coloured those areas where the component concentrations were above the average value (enriched) or above a volume fraction of 0.5 (phase separated).

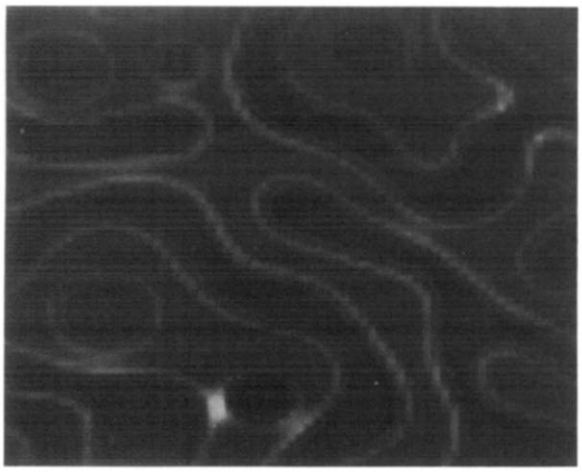

Figure 4 Phase classification cp–sc–ei. $\chi_{AB}=6$, $\chi_{AC}=3$, $\chi_{BC}=6$. $a=0.45$, $b=0.45$, $c=0.10$

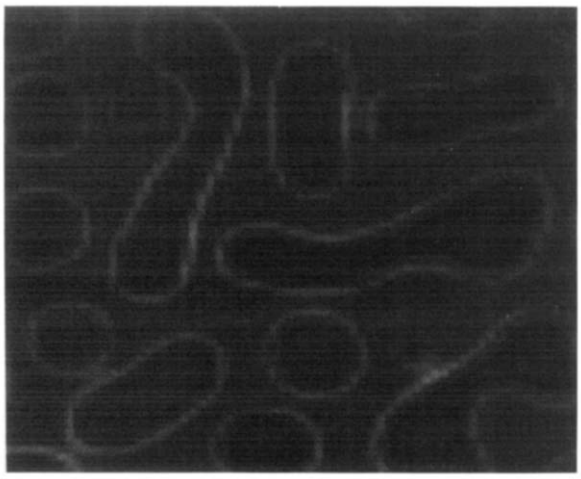

Figure 5 Phase classification cp–di–ei. $\chi_{AB}=6$, $\chi_{AC}=3$, $\chi_{BC}=6$. $a=0.50$, $b=0.40$, $c=0.10$

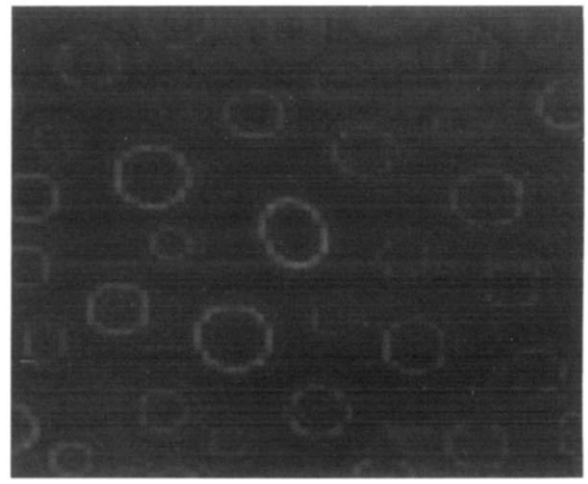

Figure 6 Phase classification cp–dc–ei, subtype (i). $\chi_{AB}=6$, $\chi_{AC}=3$, $\chi_{BC}=3$. $a=0.70$, $b=0.20$, $c=0.10$

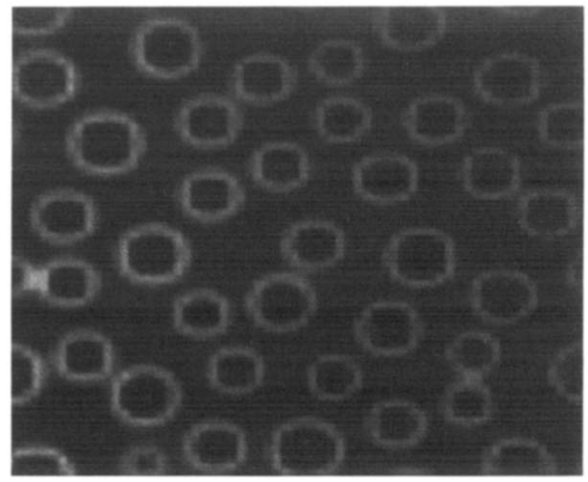

Figure 7 Phase classification cp–dc–ei, subtype (ii). $\chi_{AB}=6$, $\chi_{AC}=3$, $\chi_{BC}=6$. $a=0.70$, $b=0.20$, $c=0.10$

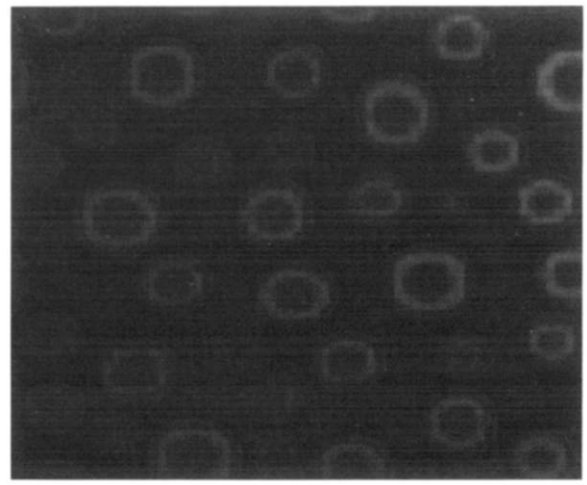

Figure 8 Phase classification cp–dc–ei, subtype (iii). $\chi_{AB}=6$, $\chi_{AC}=6$, $\chi_{BC}=3$. $a=0.70$, $b=0.20$, $c=0.10$

A third method also used separate plots for each component but with colour intensities proportional to the local concentration. This provided the best information on the spatial distribution of minor components but was ambiguous as to whether the minor component had become a separate phase. *Figures 4–9* utilize this technique.

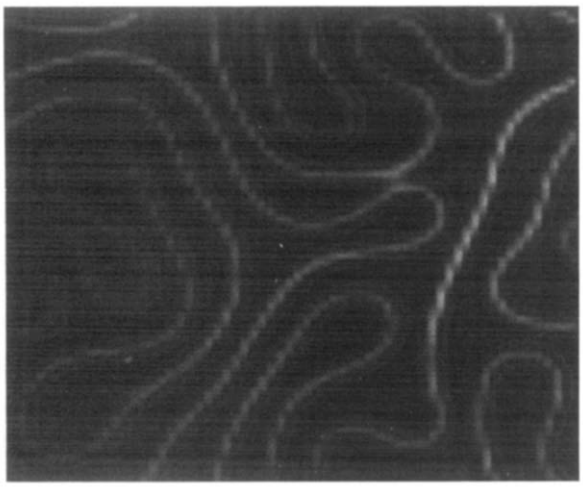

Figure 9 Phase classification sc–sc–ei, subtype (i). $\chi_{AB}=6$, $\chi_{AC}=3$, $\chi_{BC}=3$. $a=0.45$, $b=0.45$, $c=0.10$

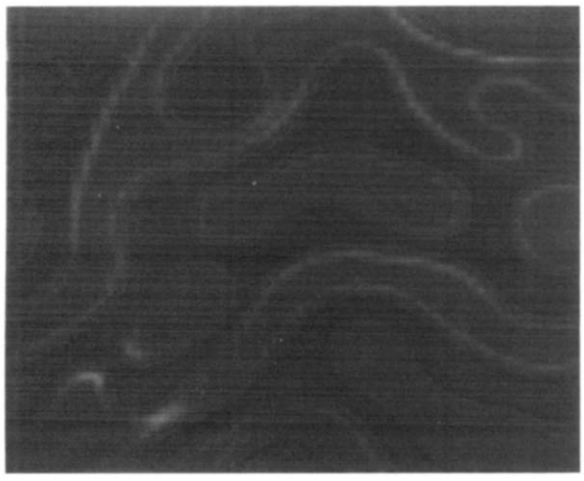

Figure 10 Phase classification sc–sc–ei, subtype (ii). $\chi_{AB}=6$, $\chi_{AC}=6$, $\chi_{BC}=3$. $a=0.50$, $b=0.40$, $c=0.10$

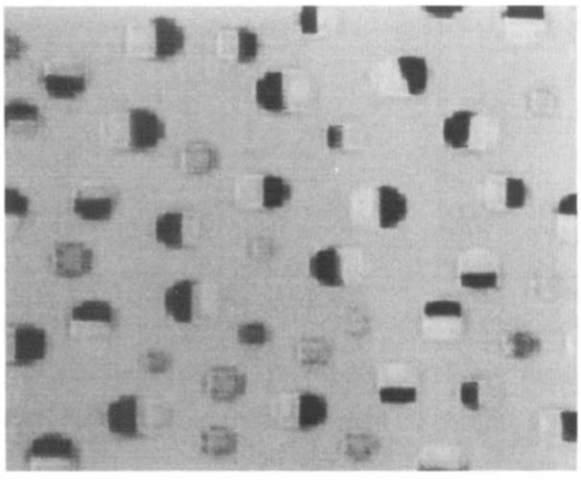

Figure 11 Phase classification cp–dc–dc, mixture of subtypes (i) and (iii). $\chi_{AB}=9$, $\chi_{AC}=9$, $\chi_{BC}=6$. $a=0.80$, $b=0.10$, $c=0.10$

Phase structures

Graphical displays of the simulation results were visually examined to determine phase structures. The following classification scheme was used.

cp The phase corresponding to this component is continuous. An uninterrupted path exists from each boundary of the simulation domain to every other boundary.

sc The phase is highly elongated and typically contacts two opposite boundaries. It is semi-continuous in two dimensions and would presumably be continuous in three dimensions.

di The phase exists as dispersed but irregular and typically elongated domains. The phase does not contact opposite boundaries.

dc The phase exists as dispersed, compact and typically circular (spherical in three dimensions) domains.

si The phase corresponding to this (typically minor) component has separated at the interface between the two other phases.

ei This component is enriched at the interface but does not appear as a separate phase.

ns There is no separate phase of this component nor is there noticeable enrichment.

A phase classification for the ternary system consists of three descriptions, one for each component. Thus cp–di–dc indicates that component A forms a continuous phase, component B forms a discrete but irregular phase and component C forms a discrete, compact phase.

A secondary set of descriptors, specifying contact between the phases, is necessary to define the morphology. In the above example of a cp–di–dc system, it may be that phase A contacts only phase B, phase B contacts phases A and C and phase C contacts only phase B. It would then be clear that phase C is contained within phase B which in turn is contained within phase A. Such morphologies are common.

RESULTS

Table 1 gives the observed morphologies for a set of 104 simulation runs in which interaction parameters and phase volumes were systematically varied. The great wealth of morphologies can be condensed to a smaller number of representative forms as defined in *Table 2* and the corresponding illustrations.

The first 56 cases in *Table 1* represent systematic permutations of volume fractions and two values of χ, $\chi_{low}=3$ and $\chi_{high}=6$. Cases 57–104 are permutations using an intermediate value of χ, $\chi_{medium}=4.5$. An additional 104 cases, not reported in detail, expanded the range of values for χ: $\chi_{low}=3$, $\chi_{medium}=6$ and $\chi_{high}=9$. The results for this expanded range are qualitatively similar to those with the limited range: $\chi_{low}=3$, $\chi_{medium}=4.5$ and $\chi_{high}=6$. Differences did arise owing to the greater extent of phase separation forced by the expanded range. Thus cases found ei in the basic study frequently became si for the expanded range. Similarly, some dc cases became di and some sc cases became cp. One new morphological type was observed, sc–di–si, and is included in *Tables 1* and *2*.

The phenomenon of minor component enrichment at the interface, between phases of the major components, is quite common. *Table 3* examines these morphologies in more detail. The illustrations corresponding to this table (*Figures 4–10*) show only the minor component and use intensities proportional to concentration. In no case does the concentration of the minor component

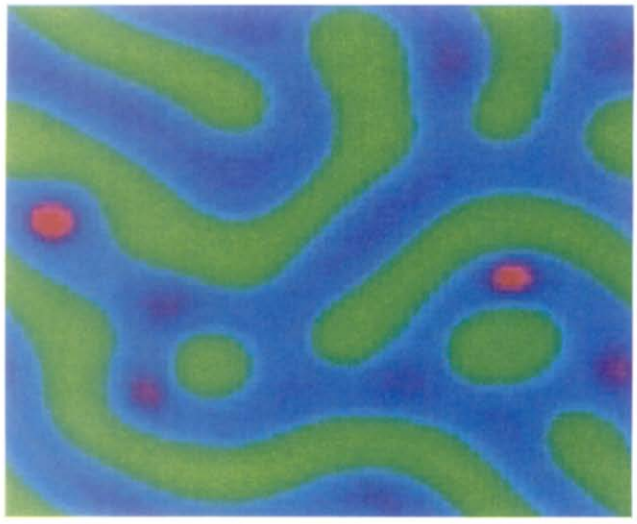

Plate 1 Phase classification cp–sc–dc. $\chi_{AB}=3$, $\chi_{AC}=3$, $\chi_{BC}=6$. $a=0.45$, $b=0.45$, $c=0.10$

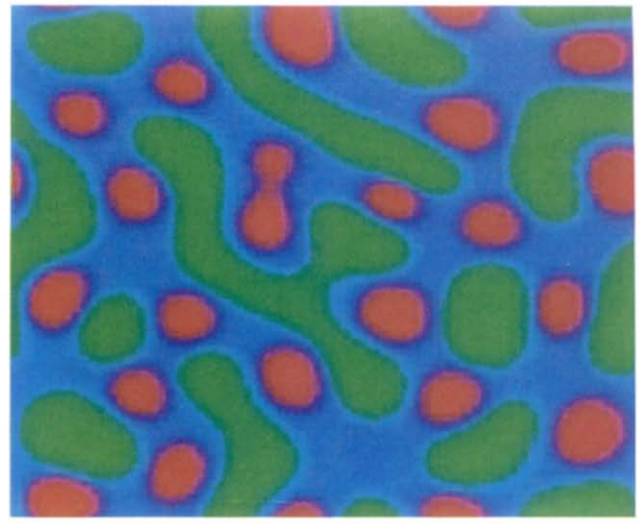

Plate 4 Phase classification cp–di–dc, subtype (ii). $\chi_{AB}=3$, $\chi_{AC}=3$, $\chi_{BC}=6$. $a=0.40$, $b=0.40$, $c=0.20$

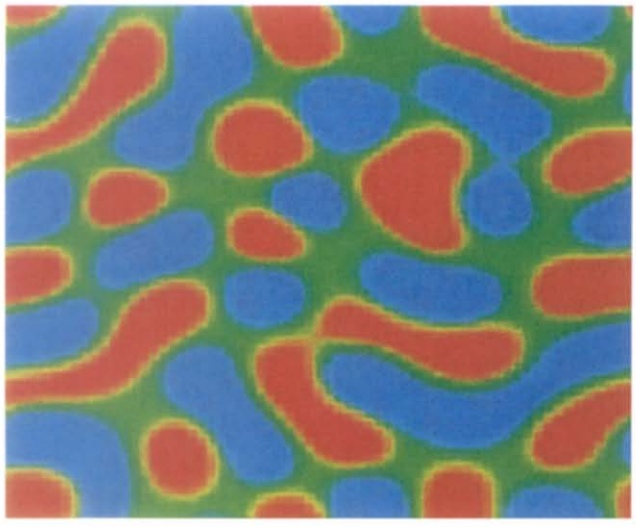

Plate 2 Phase classification cp–di–di. $\chi_{AB}=3$, $\chi_{AC}=3$, $\chi_{BC}=6$. $a=0.33$, $b=0.33$, $c=0.34$

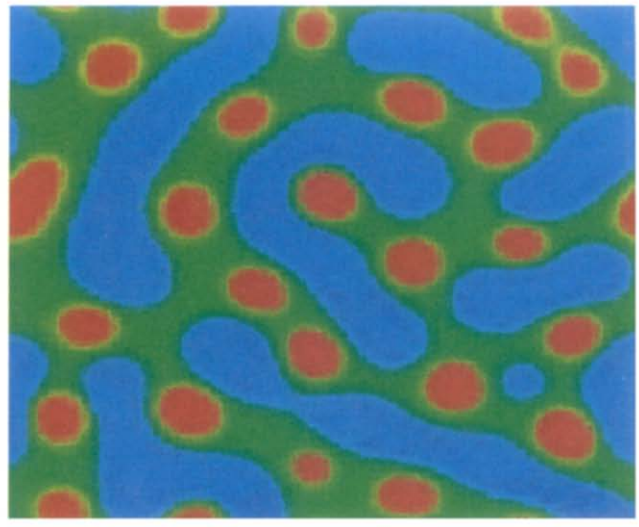

Plate 5 Phase classification cp–di–dc, subtype (iii). $\chi_{AB}=3$, $\chi_{AC}=6$, $\chi_{BC}=3$. $a=0.40$, $b=0.40$, $c=0.20$

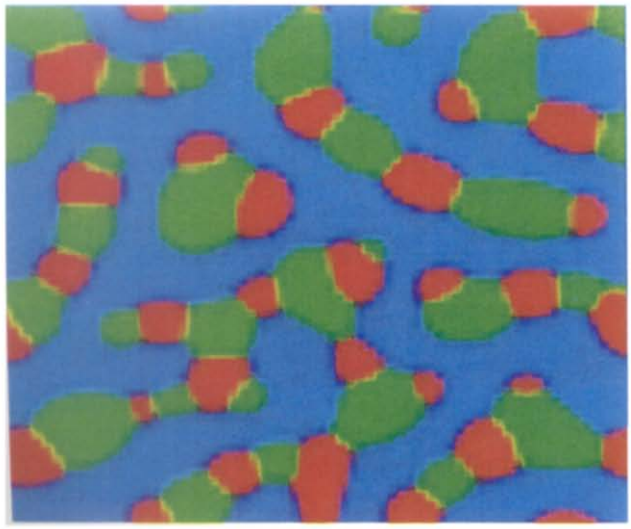

Plate 3 Phase classification cp–di–dc, subtype (i). $\chi_{AB}=6$, $\chi_{AC}=6$, $\chi_{BC}=6$. $a=0.50$, $b=0.30$, $c=0.20$

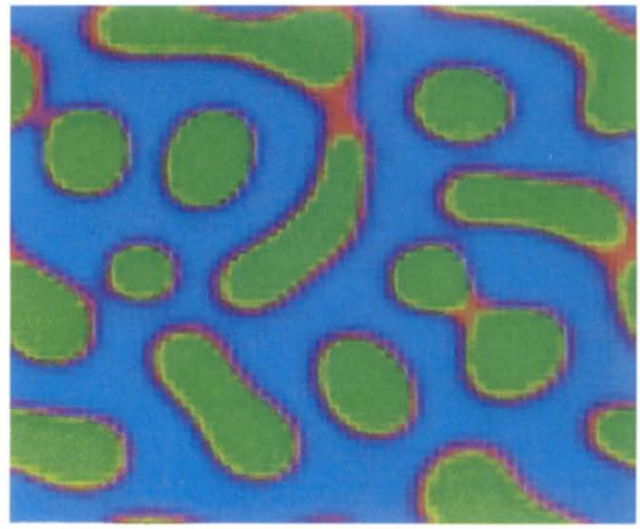

Plate 6 Phase classification cp–di–si. $\chi_{AB}=6$, $\chi_{AC}=3$, $\chi_{BC}=3$. $a=0.50$, $b=0.30$, $c=0.20$

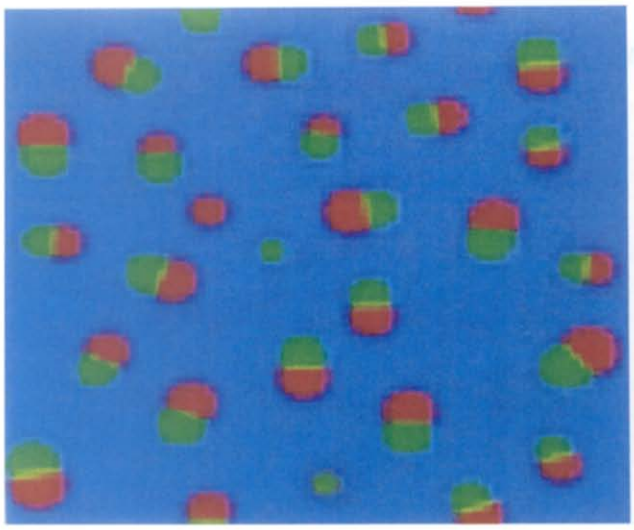

Plate 7 Phase classification cp–dc–dc, subtype (i). $\chi_{AB}=6$, $\chi_{AC}=6$, $\chi_{BC}=6$. $a=0.80$, $b=0.10$, $c=0.10$

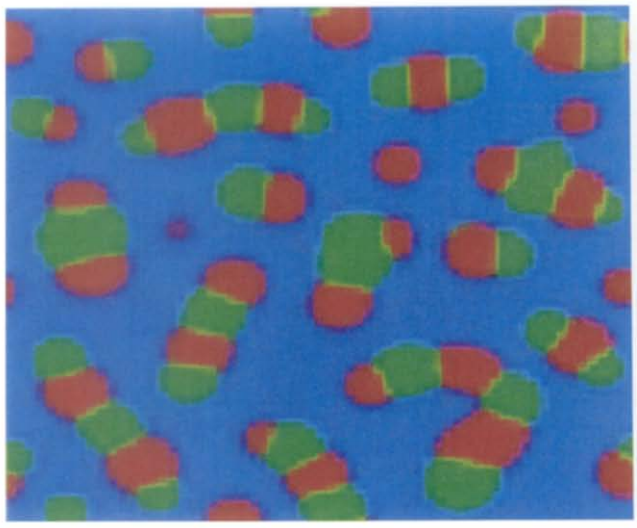

Plate 8 Phase classification cp–dc–dc, subtype (i). $\chi_{AB}=6$, $\chi_{AC}=6$, $\chi_{BC}=6$. $a=0.60$, $b=0.20$, $c=0.20$

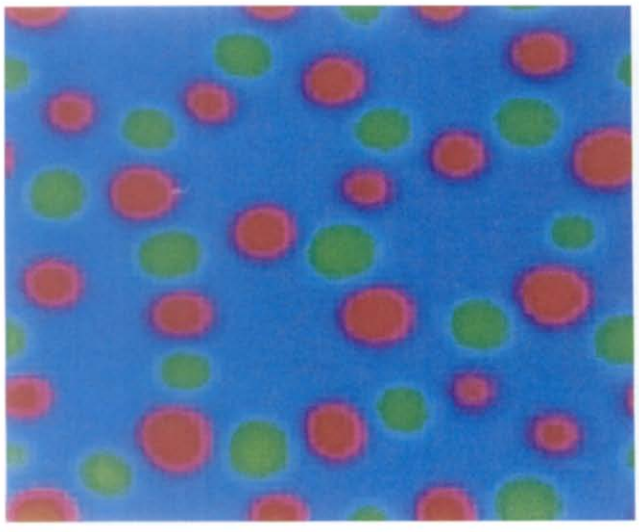

Plate 9 Phase classification cp–dc–dc, subtype (ii). $\chi_{AB}=3$, $\chi_{AC}=3$, $\chi_{BC}=6$. $a=0.60$, $b=0.20$, $c=0.20$

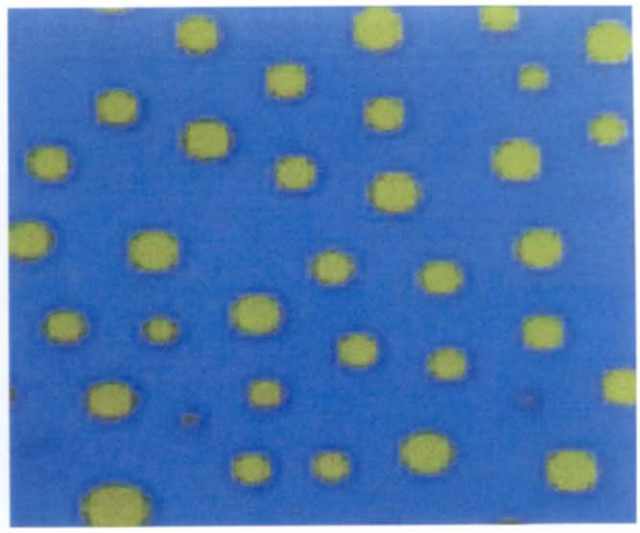

Plate 10 Phase classification cp–dc–dc, subtype (iii). $\chi_{AB}=6$, $\chi_{AC}=6$, $\chi_{BC}=3$. $a=0.80$, $b=0.10$, $c=0.10$

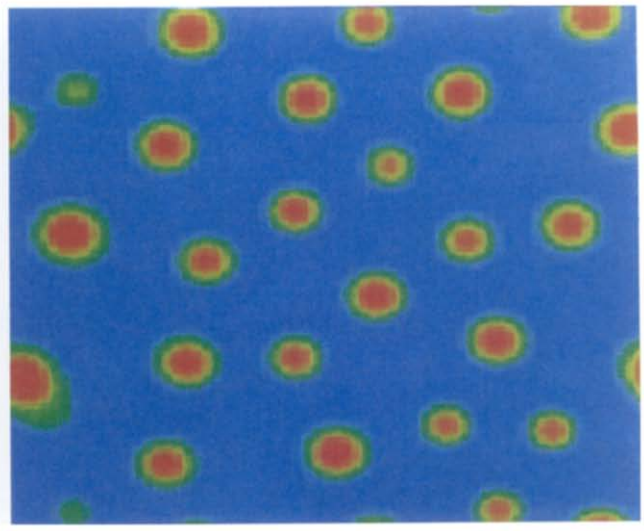

Plate 11 Phase classification cp–dc–si. $\chi_{AB}=3$, $\chi_{AC}=6$, $\chi_{BC}=3$. $a=0.70$, $b=0.20$, $c=0.10$

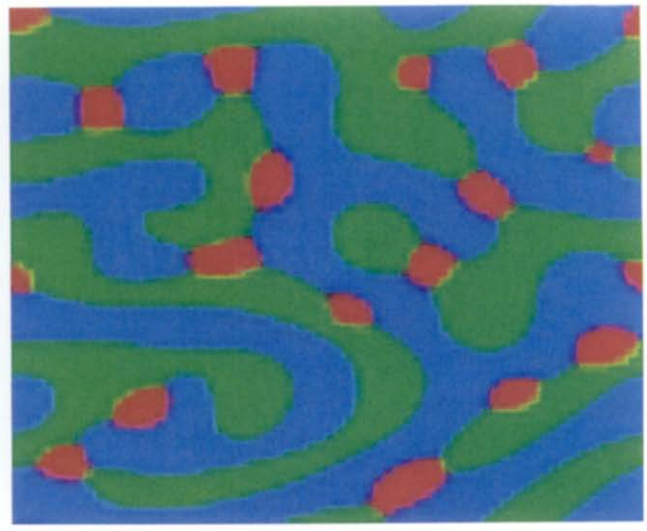

Plate 12 Phase classification sc–sc–dc, subtype (i). $\chi_{AB}=6$, $\chi_{AC}=6$, $\chi_{BC}=6$. $a=0.45$, $b=0.45$, $c=0.10$

Table 1 Morphology classifications for simulation runs

Run	χ_{AB}	χ_{AC}	χ_{BC}	A (%)	B (%)	C (%)	Morphology			Phase A contacts	Phase B contacts	Phase C contacts
							A	B	C			
1	6.0	6.0	6.0	80	10	10	cp	dc	dc	B+C	A+C	A+B
2	6.0	6.0	6.0	70	20	10	cp	dc	dc	B+C	A+C	A+B
3	6.0	6.0	6.0	60	20	20	cp	dc	dc	B+C	A+C	A+B
4	6.0	6.0	6.0	50	40	10	sc	di	dc	B+C	A+C	A+B
5	6.0	6.0	6.0	50	30	20	cp	di	dc	B+C	A+C	A+B
6	6.0	6.0	6.0	45	45	10	sc	sc	dc	B+C	A+C	A+B
7	6.0	6.0	6.0	40	40	20	di	di	dc	B+C	A+C	A+B
8	6.0	6.0	6.0	33	33	34	di	di	di	B+C	A+C	A+B
9	6.0	6.0	3.0	80	10	10	cp	dc	dc	B+C	A+C	A+B
10	6.0	6.0	3.0	70	20	10	cp	dc	ei	B	A	n.a.
11	6.0	6.0	3.0	60	20	20	cp	dc	dc	B+C	A+C	A+B
12	6.0	6.0	3.0	50	40	10	sc	sc	ei	B	A	n.a.
13	6.0	6.0	3.0	50	30	20	sc	di	di	B+C	A+C	A+B
14	6.0	6.0	3.0	45	45	10	sc	cp	ei	B	A	n.a.
15	6.0	6.0	3.0	40	40	20	di	sc	dc	B+C	A+C	A+B
16	6.0	6.0	3.0	33	33	34	dc	di	di	B+C	A+C	A+B
17	6.0	3.0	6.0	80	10	10	cp	dc	ei	B	A	n.a.
18	6.0	3.0	6.0	70	20	10	cp	dc	ei	B	A	n.a.
19	6.0	3.0	6.0	60	20	20	cp	dc	dc	B+C	A+C	A+B
20	6.0	3.0	6.0	60	20	20	cp	dc	dc	B	A	n.a.
21	6.0	3.0	6.0	50	30	20	cp	dc	dc	B+C	A+C	A+B
22	6.0	3.0	6.0	45	45	10	cp	sc	ei	B	A	n.a.
23	6.0	3.0	6.0	40	40	20	di	di	dc	B+C	A+C	A+B
24	6.0	3.0	6.0	33	33	34	di	di	di	B+C	A+C	A+B
25	6.0	3.0	3.0	80	10	10	cp	dc	ei	B	A	n.a.
26	6.0	3.0	3.0	70	20	10	cp	dc	ei	B	A	n.a.
27	6.0	3.0	3.0	60	20	20	cp	dc	si	C	C	A+B
28	6.0	3.0	3.0	50	40	10	sc	sc	ei	B	A	n.a.
29	6.0	3.0	3.0	50	30	20	cp	di	si	C	C	A+B
30	6.0	3.0	3.0	45	45	10	cp	sc	ei	B	A	n.a.
31	6.0	3.0	3.0	40	40	20	sc	sc	si	C	C	A+B
32	6.0	3.0	3.0	33	33	34	di	di	cp	C	C	A+B
33	3.0	6.0	6.0	80	10	10	cp	ei	dc	C	n.a.	A
34	3.0	6.0	6.0	70	20	10	cp	dc	dc	B+C	A+C	A+B
35	3.0	6.0	6.0	60	20	20	cp	dc	dc	B+C	A+C	A+B
36	3.0	6.0	6.0	50	40	10	sc	di	dc	B+C	A+C	A+B
37	3.0	6.0	6.0	50	30	20	cp	di	dc	B+C	A+C	A+B
38	3.0	6.0	6.0	45	45	10	sc	sc	dc	B+C	A+C	A+B
39	3.0	6.0	6.0	40	40	20	di	di	dc	B+C	A+C	A+B
40	3.0	6.0	6.0	33	33	34	di	di	dc	B+C	A+C	A+B
41	3.0	6.0	3.0	80	10	10	cp	ei	dc	C	n.a.	A
42	3.0	6.0	3.0	70	20	10	cp	si	dc	B	A+C	B
43	3.0	6.0	3.0	60	20	20	cp	si	dc	B	A+C	B
44	3.0	6.0	3.0	50	40	10	sc	sc	dc	B	A+C	B
45	3.0	6.0	3.0	50	30	20	cp	di	dc	B	A+C	B
46	3.0	6.0	3.0	45	45	10	di	cp	dc	B	A+C	B
47	3.0	6.0	3.0	40	40	20	di	cp	dc	B	A+C	B
48	3.0	6.0	3.0	33	33	34	di	cp	di	B	A+C	B
49	3.0	3.0	6.0	80	10	10	cp	ns	ns	n.a.	n.a.	n.a.
50	3.0	3.0	6.0	70	20	10	cp	ns	ns	n.a.	n.a.	n.a.
51	3.0	3.0	6.0	60	20	20	cp	dc	dc	B+C	A	A
52	3.0	3.0	6.0	50	40	10	cp	di	ns	B	A	n.a.
53	3.0	3.0	6.0	50	30	20	cp	dc	dc	B+C	A	A
54	3.0	3.0	6.0	45	45	10	cp	sc	sc	B+C	A	A
55	3.0	3.0	6.0	40	40	20	cp	di	dc	B+C	A	A

continued

Table 1 *continued*

Run	χ_{AB}	χ_{AC}	χ_{BC}	A (%)	B (%)	C (%)	Morphology A	Morphology B	Morphology C	Phase A contacts	Phase B contacts	Phase C contacts
56	3.0	3.0	6.0	33	33	34	cp	di	di	B+C	A	A
57	6.0	4.5	3.0	80	10	10	cp	dc	ei	B	A	n.a.
58	6.0	4.5	3.0	70	20	10	cp	dc	ei	B	A	n.a.
59	6.0	4.5	3.0	60	20	20	cp	dc	si	C	C	A+B
60	6.0	4.5	3.0	50	40	10	sc	sc	ei	B	A	n.a.
61	6.0	4.5	3.0	50	30	20	sc	di	di	B+C	A+C	A+B
62	6.0	4.5	3.0	45	45	10	sc	sc	ei	B	A	n.a.
63	6.0	4.5	3.0	40	40	20	di	di	dc	B+C	A+C	A+B
64	6.0	4.5	3.0	33	33	34	di	di	di	B+C	A+C	A+B
65	6.0	3.0	4.5	80	10	10	cp	dc	ei	B	A	n.a.
66	6.0	3.0	4.5	70	20	10	cp	dc	di	B	A	n.a.
67	6.0	3.0	4.5	60	20	20	cp	dc	di	C	C	A+B
68	6.0	3.0	4.5	50	40	10	cp	di	ei	B	A	n.a.
69	6.0	3.0	4.5	50	30	20	cp	di	ei	C	C	A+B
70	6.0	3.0	4.5	45	45	10	cp	sc	ei	B	A	n.a.
71	6.0	3.0	4.5	40	40	20	sc	di	di	C	C	A+B
72	6.0	3.0	4.5	33	33	34	di	dc	di	B+C	A+C	A+B
73	4.5	6.0	3.0	80	10	10	cp	ei	dc	C	n.a.	A
74	4.5	6.0	3.0	70	20	10	cp	si	dc	B+C	A+C	B
75	4.5	6.0	3.0	60	20	20	cp	si	dc	B	A+C	B
76	4.5	6.0	3.0	50	40	10	sc	cp	ns	B	A	n.a.
77	4.5	6.0	3.0	50	30	20	sc	di	dc	B+C	A+C	A+B
78	4.5	6.0	3.0	45	45	10	sc	cp	ns	B	A	n.a.
79	4.5	6.0	3.0	40	40	20	di	sc	dc	B+C	A+C	A+B
80	4.5	6.0	3.0	33	33	34	dc	di	di	B+C	A+C	A+B
81	4.5	3.0	6.0	80	10	10	cp	ns	ns	n.a.	n.a.	n.a.
82	4.5	3.0	6.0	70	20	10	cp	dc	ns	B	A	n.a.
83	4.5	3.0	6.0	60	20	20	cp	dc	ns	B	A	n.a.
84	4.5	3.0	6.0	50	40	10	cp	di	ns	B	A	n.a.
85	4.5	3.0	6.0	50	30	20	cp	dc	dc	B+C	A	A
86	4.5	3.0	6.0	45	45	10	cp	sc	ns	B	A	A
87	4.5	3.0	6.0	40	40	20	cp	di	dc	B+C	A+C	A+B
88	4.5	3.0	6.0	33	33	34	di	dc	di	B+C	A+C	A+B
89	3.0	6.0	4.5	80	10	10	cp	si	dc	C	n.a.	A
90	3.0	6.0	4.5	70	20	10	cp	si	dc	B	A+C	B
91	3.0	6.0	4.5	60	20	20	cp	si	dc	B	A+C	B
92	3.0	6.0	4.5	50	40	10	cp	di	dc	B+C	A+C	A+B
93	3.0	6.0	4.5	50	30	20	cp	di	dc	B	A+C	B
94	3.0	6.0	4.5	45	45	10	sc	sc	dc	B	A	B
95	3.0	6.0	4.5	40	40	20	di	di	dc	B	A	B
96	3.0	6.0	4.5	33	33	34	di	di	di	B	A	B
97	3.0	4.5	6.0	80	10	10	cp	ns	ns	n.a.	n.a.	n.a.
98	3.0	4.5	6.0	70	20	10	cp	ns	ns	n.a.	n.a.	n.a.
99	3.0	4.5	6.0	60	20	20	cp	ns	dc	C	n.a.	A
100	3.0	4.5	6.0	50	40	10	cp	di	ns	B	A	n.a.
101	3.0	4.5	6.0	50	30	20	sc	dc	dc	B+C	A+C	A+B
102	3.0	4.5	6.0	45	45	10	sc	di	dc	B+C	A+C	A+B
103	3.0	4.5	6.0	40	40	20	sc	di	dc	B+C	A+C	A+B
104	3.0	4.5	6.0	33	33	34	di	di	dc	B+C	A+C	A+B
111	9.0	6.0	3.0	40	40	20	di	sc	si	C	C	A+B
155	6.0	6.0	6.0	60	20	20	cp	dc	dc	B+C	A+C	A+B
169	9.0	9.0	6.0	80	10	10	cp	dc	dc	B+C	A+C	A+B

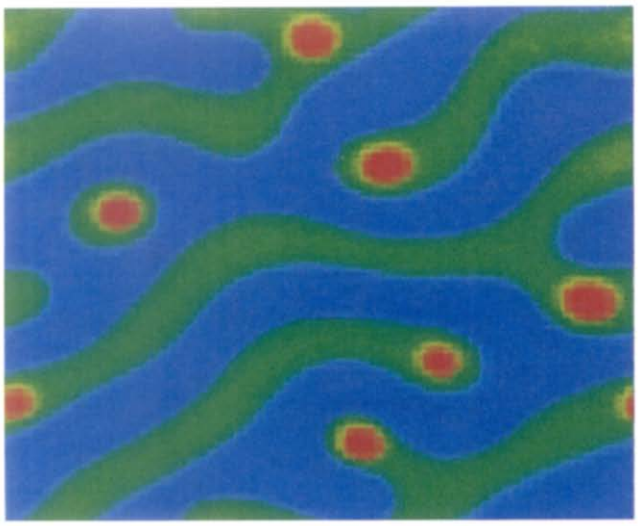

Plate 13 Phase classification sc–sc–dc, subtype (ii). $\chi_{AB}=3$, $\chi_{AC}=6$, $\chi_{BC}=3$. $a=0.50$, $b=0.40$, $c=0.10$

Plate 14 Phase classification sc–sc–si. $\chi_{AB}=6$, $\chi_{AC}=3$, $\chi_{BC}=3$. $a=0.40$, $b=0.40$, $c=0.20$

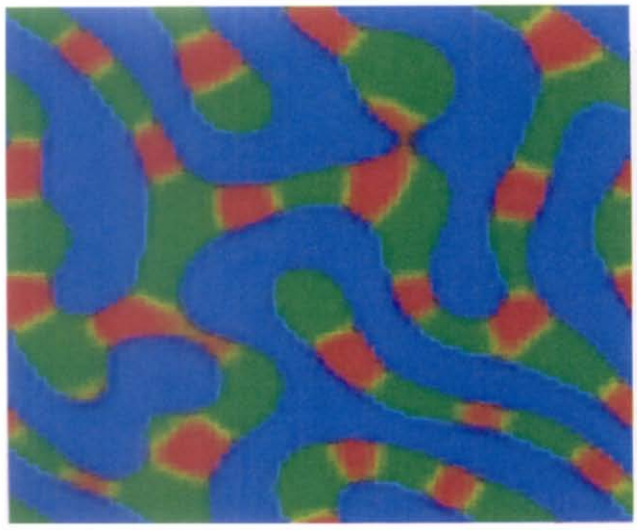

Plate 15 Phase classification sc–di–di. $\chi_{AB}=6$, $\chi_{AC}=6$, $\chi_{BC}=3$. $a=0.50$, $b=0.30$, $c=0.20$

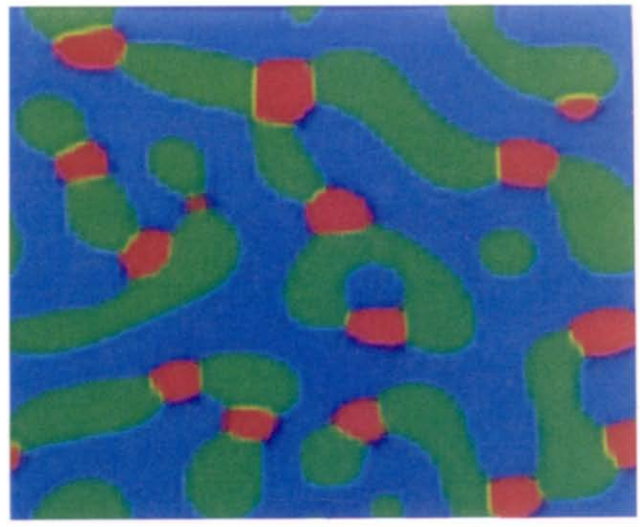

Plate 16 Phase classification sc–di–dc, subtype (i). $\chi_{AB}=6$, $\chi_{AC}=6$, $\chi_{BC}=6$. $a=0.50$, $b=0.40$, $c=0.10$

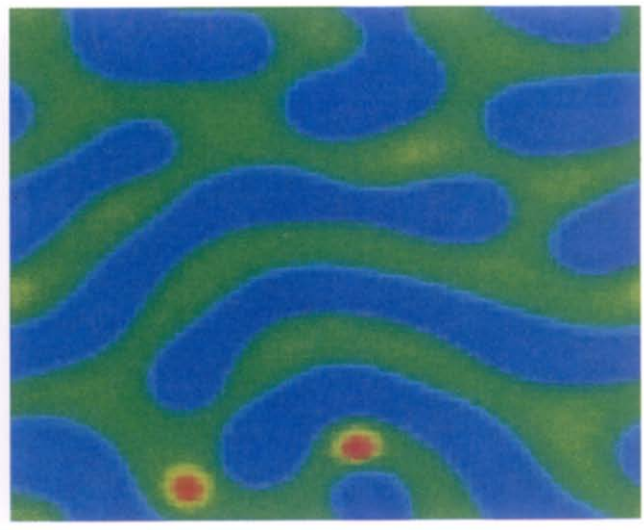

Plate 17 Phase classification sc–di–dc, subtype (ii). $\chi_{AB}=3$, $\chi_{AC}=6$, $\chi_{BC}=3$. $a=0.45$, $b=0.45$, $c=0.10$

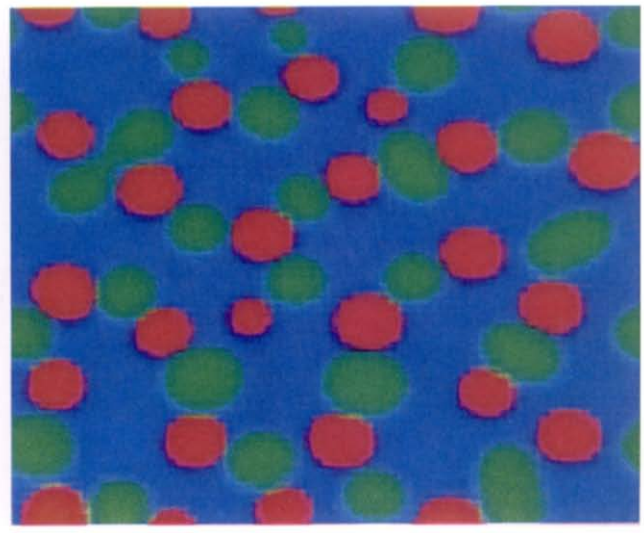

Plate 18 Phase classification sc–dc–dc. $\chi_{AB}=3$, $\chi_{AC}=4.5$, $\chi_{BC}=6$. $a=0.50$, $b=0.30$, $c=0.20$

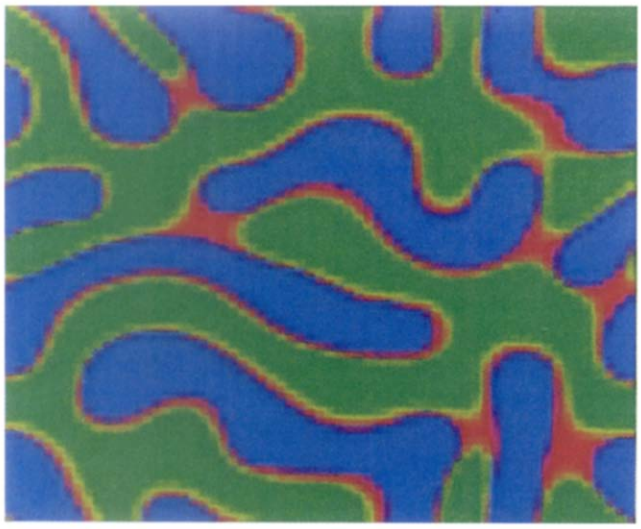

Plate 19 Phase classification sc–di–si. $\chi_{AB}=9$, $\chi_{AC}=6$, $\chi_{BC}=3$. $a=0.40$, $b=0.40$, $c=0.20$

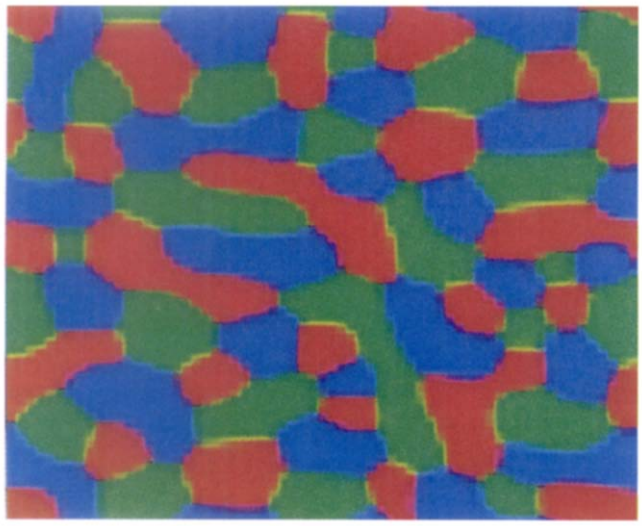

Plate 20 Phase classification di–di–di. $\chi_{AB}=6$, $\chi_{AC}=6$, $\chi_{BC}=6$. $a=0.33$, $b=0.33$, $c=0.34$

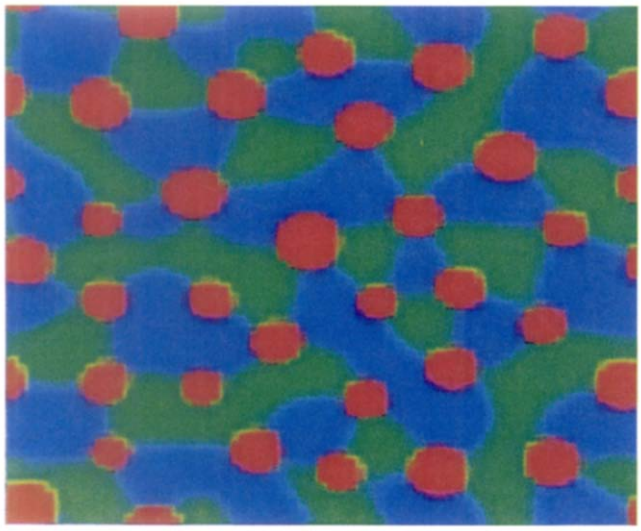

Plate 21 Phase classification di–di–dc. $\chi_{AB}=3$, $\chi_{AC}=6$, $\chi_{BC}=6$. $a=0.40$, $b=0.40$, $c=0.20$

exceed 50%. Note that the minor component may show a preference for one of the phases.

DISCUSSION

The results illustrate a wealth of two-dimensional morphologies that can result from the spinodal decomposition of ternary polymer blends. The present paper does not attempt to specify rules under which a particular morphology will be obtained. However, some simple generalizations are possible.

The volume fractions of the components are more important in determining morphology than the χ. A component with a volume fraction of 0.6 or higher always formed a continuous phase while no continuous phase was observed with a volume fraction less than 0.33. Semicontinuity was confined to the range 0.3–0.5 and the dispersed, irregular morphology was confined to the range 0.2–0.45. The dispersed, compact morphology was not observed at volume fractions above 0.34, and a separated phase at the interface was not observed at volume fractions above 0.2.

Components comprising less than 20 vol% of a three-phase mixture formed either dc or si phases. The si morphology was observed for component C when χ_{AB} was greater than χ_{AC} and χ_{BC}. Similarly, the si morphology was observed for component B when χ_{AC} was greater than χ_{BC} and χ_{AB}. Components that formed si phases at concentrations of 10 and 20% formed a continuous phase when all three components were present in equal amounts. These cases showed interfacial enrichment when the minor component was too low in concentration to develop as a separate si phase.

The system with $\chi_{AB}=6$, $\chi_{AC}=\chi_{BC}=3$ approximated the situation where minor component C is a block copolymer of components A and B. This system showed the ei or si morphologies except for $\bar{c}=0.34$, where the C phase became continuous. Note, however, that this simple approximation cannot predict the internal structure within a block copolymer phase.

The case where two dispersed, compact phases are mutually avoiding within a continuous phase (cp–dc–dc, subtype (ii)) is comparatively rate. The usual situation is for the minor phases to contact each other so that interfacial area is minimized. Thus $\chi_{AB}=6$, $\chi_{AC}=6$, $\chi_{BC}=9$ with $\bar{b}=\bar{c}=0.2$ showed touching B and C phases despite the high value for χ_{BC} and despite the fact that $\chi_{AB}=3$, $\chi_{AC}=3$, $\chi_{BC}=6$ (run 51) is the type specimen for the mutually avoiding case.

As discussed previously, it is believed that most of the simulation results are in the scaling region in which the morphology, is invariant with time despite interphase diffusion (Ostwald ripening). However, the present study has not confirmed this belief numerically and it is clear that some of the morphologies will change at sufficiently long times. Thus the mixed, quasiphase found in cp–dc–dc, subtype (iii), will be unstable and will eventually bifurcate into the cp–dc–dc, subtype (i), structure. *Figure 11* illustrates this phenomenon by showing a cp–dc–dc morphology that is a mixture of subtypes (i) and (iii). Some of the si and ei morphologies may also be unstable under prolonged spinodal decomposition.

The morphologies possible in two-phase systems are quite limited. The forms cp–sc, cp–di, cp–dc and sc–sc were observed for cases where the third component did not form a separate phase.

Table 2 Type specimens for observed morphologies in three-phase systems

Phase classification	Type specimen		Discussion
	Run no.	Plate no.	
cp–sc–di			Not observed
cp–sc–dc	54	*1*	The sc phase does not contact opposite boundaries but otherwise appears semicontinuous
cp–sc–si			Not observed
cp–di–di	48	*2*	All examples have isolated di phases that contact only the cp
cp–di–dc	5(i) 55(ii) 47(iii)	*3* *4* *5*	This morphology has three subtypes: (i) the phases are mutually contacting; (ii) the di and dc phases are mutually avoiding; (iii) the dc phase is contained within the cp phase
cp–di–si	29	*6*	This is an elongated form of the core–shell morphology
cp–dc–dc	1, 3(i) 51(ii) 9(iii)	*7, 8* *9* *10*	This morphology has three subtypes: (i) the phases are mutually contacting, the two type specimens differ in degree; (ii) the dc phases are mutually avoiding; (iii) the two minor components have formed a mixed, quasi-phase
cp–dc–si	42	*11*	This is the core–shell morphology in its classical form
sc–sc–di			Not observed
sc–sc–dc	6(i) 44(ii)	*12* *13*	Two subtypes have been observed: (i) the phases are mutually contacting; (ii) the dc phase is contained within one of the sc phases
sc–sc–si	31	*14*	A fully separated minor phase exists at all points along the convoluted interface
sc–di–di	13	*15*	The distinctions between this form and the sc–di–dc and sc–dc–dc forms is more of degree than kind. The sc–di–dc form is the most common
sc–di–dc	4(i) 46(ii)	*16* *17*	Two subtypes have been observed: (i) the phases are mutually contacting, the type specimen has chains of alternating di and dc units; (ii) the dc phase is contained within the sc phase
sc–dc–dc	101	*18*	The dc phases alternate in long chains similar to sc–di–dc, subtype (i). The sc phase is nearly continuous but connectivity is blocked by 'no phase' regions between domains
sc–di–si	111	*19*	A separated phase occupies the interface
sc–dc–si			Not observed
di–di–di	8	*20*	The phases are mutually contacting
di–di–dc	39	*21*	The phases are mutually contacting
di–di–si	Not observed. These and the following forms are theoretically possible with two- or three-dimensional space-filling shapes. However, such shapes have not been observed to result from spinodal decomposition.		
di–dc–dc	Not observed		
di–dc–si	Not observed		
dc–dc–dc	Not observed		
dc–dc–si	Not observed		

Table 3 Type specimens for observed morphologies in two-phase systems with enrichment

Phase classification	Type specimen		Discussion
	Run no.	Figure no.	
cp–sc–ei	22	*4*	The type specimen shows enrichment at the interface. This particular specimen also shows a preference by the enriched component for the continuous phase
cp–di–ei	20	*5*	The type specimen shows enrichment at the interface and preference by the enriched component for the continuous phase
cp–dc–ei	26(i) 18(ii) 10(iii)	*6* *7* *8*	The three subtypes show: (i) no preference; (ii) a continuous phase preference; (iii) a discontinuous phase preference by the enriched component
sc–sc–ei	30(i) 12(ii)	*9* *10*	The two subtypes show: (i) no preference; (ii) a preference for one phase by the enriched component

CONCLUSIONS

This paper has presented a taxonomy of phase structures in ternary polymer blends. The predicted two-dimensional structures are directly testable using films cast from ternary polymer mixtures in a common, compatibilizing solvent. In this regard, the morphology in *Figure 1* has the sc–sc structure expected in a two-dimensional, two-phase mixture with commensurate volume fractions of the two phases. *Figure 2* exhibits an sc–sc–dc, subtype (ii), structure at volume fractions nearly identical to the type specimen, run 44 (*Plate 13*). *Figure 3* appears to show a cp–dc–si structure although at a volume fraction for the dispersed phase which is substantially higher than that for the type specimen, run 42 (*Plate 11*).

In principle, the taxonomy can be applied to two-dimensional cuts from bulk, three-dimensional samples as prepared by compositional quenching. All sc structures and some of the di structures would be fully continuous owing to the extra degree of connectivity in three dimensions. Thus morphologies such as cp–sc–*xx* and sc–sc–*xx* would have two continuous phases. In practice, however, it has been found difficult to prepare bulk samples with co-continuity[4,14]. Thus, observed morphologies may be confined to forms having one continuous phase and one or two dispersed phases.

Even with the potentially restricted morphologies achievable in three dimensions, there remain multiphase materials of commercial importance. Morphologies such as cp–dc–ei and cp–dc–si reflect the addition of a compatibilizing agent (e.g. maleated polyethylene in a matrix of poly(ethylene terephthalate) with polyethylene as a dispersed phase). The results and methodology presented here should be useful for establishing volume fractions appropriate to the three polymers.

If co-continuity is unstable in three dimensions, morphologies such as cp–dc–dc, subtype (ii), will be more common than in films. Such materials could have commercial advantages compared to the usual two-phase system with cp–dc morphology. If, for example, the two dc phases are rubbers having significantly different interaction parameters with the matrix phase, it may be possible to create bimodal particle size distributions.

ACKNOWLEDGEMENT

Figures 1, 2 and *3* were obtained by Dr Murali V. Ariyapadi.

REFERENCES

1 Kresge, E. N. in 'Polymer Blends' (Eds D. R. Paul and S. Newman), Vol. II, Academic Press, New York, 1978
2 Nauman, E. B., Airyapadi, M. V., Balsara, N. P., Grocela, T. A., Furno, J. S., Liu, S. H. and Mallikarjun, R. *Chem. Eng. Commun.* 1988, **66**, 29
3 Siggia, E. D. *Phys. Rev.* 1979, **A20** (2), 595
4 Rousar, I. and Nauman, E. B. *Chem. Eng. Commun.* 1991, **105**, 77
5 Vasishta, N. and Nauman, E. B. *Proc. Am. Chem. Soc. Div. Polym. Mater.* 1993, **69**, 168
6 Nauman, E. B. and Balsara, N. *Fluid Phase Equilib.* 1988, **45**, 229
7 Nauman, E. B., Rousar, I. and Dutta, A. *Chem. Eng. Commun.* 1991, **105**, 61
8 Cussler, E. L. 'Diffusion, Mass Transfer in Fluids Systems', Cambridge University Press, 1984
9 Cahn, J. W. and Hilliard, J. E. *J. Chem. Phys.* 1958, **28** (2), 258
10 Ariyapadi, M. V. and Nauman, E. B. *J. Polym. Sci., Polym. Phys. Edn* 1990, **28**, 2395
11 de Gennes, P. G. *J. Chem. Phys.* 1981, **72** (9), 4756
12 Scott, R. L. *J. Chem. Phys.* 1949, **17** (3), 279
13 Tompa, H. *Trans. Faraday Soc.* 1949, **45**, 1142
14 Grocela, T. A. Doctoral Dissertation, Rensselaer Polytechnic Institute, Troy, NY, 1992